# Multiobjective Optimization of Radar Acquisition Parameters in Flyby Scenarios of Planetary Missions

Alberto Frizzera, Massimo Santoni, and Lorenzo Bruzzone, *Fellow, IEEE*

***Abstract*— In planetary explorations, missions that employ flybys operate in strongly variable environments. The rapid change in altitude of a flyby orbit increases the difficulties in determining the optimal instrument parameters to properly study the investigated celestial body. Typically, the selection of the parameters is guided by multiple criteria according to the mission's scientific objectives and the available resources. In this letter, we propose a novel automatic strategy to find the optimal instrument configuration exploiting a multiobjective optimization. The problem is addressed as the minimization of an objective function, which evaluates the acquisition properties. Thus, the solutions represent the best trade-offs between system performance and resource consumption. We tested our approach on a monostatic radar sounder (RS) capable of penetrating and analyzing the celestial bodies' subsurface. In particular, we considered the Radar for Icy Moon Exploration (RIME) on board the JUpiter Icy moons Explorer (JUICE) that will study the Jovian moons: Europa, Ganymede, and Callisto. Several planning simulations have been conducted, considering numerous flybys on the three moons while adopting signal-to-noise ratio (SNR), data rate, and orbit uncertainty as objectives. Results confirmed the effectiveness of the proposed approach, reaching a surface SNR of 60 dB with a data rate of 9 Mb/s for the 7E1 flyby on Europa.**

***Index Terms*— Flyby, optimization, radar sounder (RS), Radar for Icy Moon Exploration (RIME).**

## I. Introduction

IN RECENT years, from the inner to the outer solar systems, several missions have been developed to study and characterize the structure of celestial bodies. Modern spacecrafts usually include different kinds of instruments to analyze the properties of a given target. Each instrument has to be carefully configured, taking into account the working environment and the acquisition geometry. Consequently, the relative position between the orbit and the target plays a pivotal role in determining the correct instrument parameters, especially when active measurements are considered. In circular orbits, since the altitude is almost constant, the parameters are usually manually selected and kept unchanged during the acquisition [1], [2]. Differently, while considering flybys, the altitude has fast nonlinear variations, making the selection of the parameters more challenging.

In this letter, we focus our attention on the selection of the parameters during flybys, therefore adopting complex operational scenarios. We assume to work with instruments whose measurements highly depend on the spacecraft velocity and altitude. In such cases, the constraints given by the acquisition geometry change over the flyby, defining a dynamic region of feasibility, which is often not easy to explore. Furthermore, the parameters have to be chosen, taking into account the mission objectives and the available resources. Accordingly, the solutions should represent an optimal compromise among the mission requirements, ensuring high system performance with low resource consumption. Therefore, we formulate the problem as a constrained multiobjective optimization that should be addressed with proper efficient strategies. Although the problem formulation is valid for numerous instruments, such as laser altimeters, radar for imaging, or radar sounders (RSs), in this letter, we focus on RS applications.

RSs proved to be very effective in generating radargrams, which enable us to understand past and present geological activity and contribute to the analysis of the chemical composition of the target's subsurface. In space contexts, we usually refer to RSs as monostatic systems, which employ the SAR strategy for azimuth compression on the along-track direction. This technology implies a strict design of the radar timeline, which has to include the wave time-of-flight (ToF), the nonoverlapping transmission and receiving windows, and a safety margin. In addition, RSs usually adopt multiple-rank transmissions to increase the number of pulses and improve the data quality. When the altitude leads to a high ToF, the radar sends multiple pulses before receiving the first one. In this manner, the waiting time is minimized, and the instrument's capabilities are better exploited. The timeline constraints and the multiple-rank concept define a more complex optimization problem without a unique analytical solution. For this reason, an automatic method to set up the instrument parameters, taking into account mission constraints, is required.

We propose an approach to the automatic selection of the best trade-offs among radar parameters and mission resources based on multiobjective optimization. The problem is described by a 1-D vector and then solved with the minimization of three specific performance metrics, which are comprehensively explained in Section III. Even if the problem and the proposed solution are general in radar systems, in this

Manuscript received 21 February 2024; revised 21 May 2024 and 6 June 2024; accepted 16 July 2024. Date of publication 24 July 2024; date of current version 9 August 2024. This work was supported by Italian Space Agency ("Attività di Ground Segment per lo strumento Radar for Icy Moon Exploration (RIME) della missione JUpiter Icy moons Explorer (JUICE) di European Space Agency (ESA)," CUP F65F21000950005) under Contract 2021-21-HH.0. *(Corresponding author: Lorenzo Bruzzone.)*

The authors are with the Department of Information Engineering and Computer Science Trento, University of Trento, 38123 Trento, Italy (e-mail: lorenzo.bruzzone@unitn.it).

Digital Object Identifier 10.1109/LGRS.2024.3433000

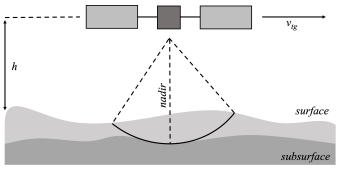


Fig. 1. Illustration of the acquisition geometry of an RS.

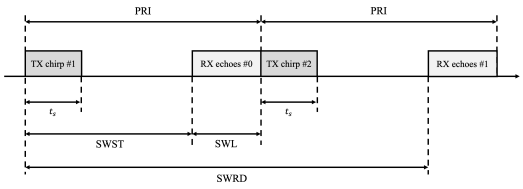


Fig. 2. Radar timeline considering the transmission at rank = 1.

letter, we focus on the Radar for Icy Moon Exploration (RIME) [3], an instrument operating at a central frequency of 9 MHz with a bandwidth up to 2.8 MHz, on board the JUpiter Icy moons Explorer (JUICE) [4]. JUICE will study the Jupiter system and, in particular, three of the Galilean icy moons: Europa, Ganymede, and Callisto. On the three bodies, several flybys will be performed with the closest approaches at an altitude below 1000 km.

## II. Background and Problem Formulation

The reference scenario, represented in Fig. 1, consists of a nadir-looking RS that employs the SAR focusing in the along-track direction. We assume to work with a single antenna that performs transmission or receiving by sending chirp pulses to increase the range resolution.

As introduced in Section I, the radar timeline has to include the wave ToF at the given altitude, the nonoverlapping transmission and receiving windows, and a safety margin due to the orbit uncertainty. More in detail, we consider a fixed pulsewidth ($t_s$) as the transmission window and a variable receiving window denoted as the sampling window length (SWL). The SWL should be defined, so that all the echoes coming from the subsurface are collected; thus, it is strictly correlated with the maximum achievable penetration depth. Due to some uncertainties related to the ground permittivity as well as the orbit position, the echoes could be anticipated or delayed. For this reason, it is necessary to add to the SWL a safety margin, which we call altitude margin, as it mainly refers to the altitude knowledge uncertainty of the spacecraft. The altitude margin can also be converted into a quantity that measures the probability that all the echoes remain within the SWL. The SWL is defined as follows:

$$\mathrm{SWL} = \frac{2}{c}(D_p \cdot \sqrt{\epsilon_r} + m_h) + t_s \tag{1}$$

where $D_p$ is the penetration depth and $m_h$ is the altitude margin. Fig. 2 illustrates the radar timeline with the involved design variables. Considering the transmission at multiple ranks, we define the sampling window real delay (SWRD) as the time interval that measures the two-way ToF of a pulse reflected by the surface, so it includes only the spacecraft

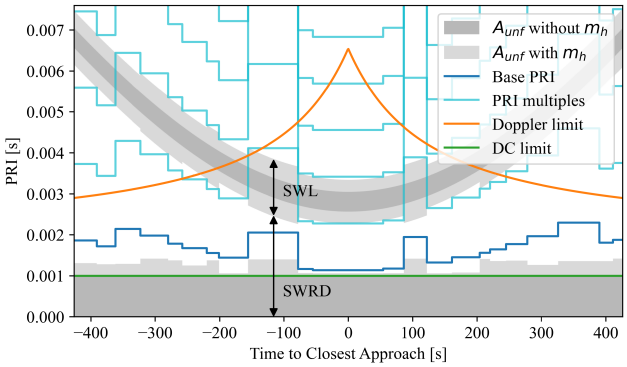


Fig. 3. Graphical explanation of the condition to have valid PRIs. The multiples of the base PRI (first pulse PRI) must not overlay the unfeasible region ($A_{\mathrm{unf}}$) also including the altitude margin (light gray). In addition, the base PRI must be contained in the range between the duty cycle and the Doppler limits. The altitude margin is a variable associated with the risk of losing part of the received signal and is part of the optimization; thus, it may change in different PRI segments and is spread before and after the ideal SWL. Note that the margin belonging to the SWL of the first PRI is partially visible, since it is covered by the dc limit.

altitude ($h$) without the penetration depth

$$\mathrm{SWRD} = \frac{2}{c}\left(h - \frac{m_h}{2}\right). \tag{2}$$

The sampling window start time (SWST) instead indicates the time between the start of the transmission and receiving windows within one pulse repetition interval (PRI). Note that when rank = 0, the SWST is equal to the SWRD, whereas at multiple ranks, the SWST loses a physical meaning and simply informs the instrument when to start sampling. SWST and SWRD are connected by the following relation:

$$\mathrm{SWST} = \mathrm{SWRD} - \mathrm{rank} \cdot \mathrm{PRI}. \tag{3}$$

To avoid overlapping between transmission and receiving, the PRI has to be carefully selected. The necessary and sufficient condition to have a valid PRI can be formulated as follows:

$$\begin{gathered} \forall\ \mathrm{rank} \in [1, r_{\max}] \\ \mathrm{rank} \cdot \mathrm{PRI} \notin [\mathrm{SWRD} - t_s, \mathrm{SWRD} + \mathrm{SWL}]. \end{gathered} \tag{4}$$

In other words, the next transmission with the selected PRI (identified as base PRI) must not be performed during the receiving of the first transmitted pulse that is delayed, since we are considering multiple ranks. Thus, for each pulse, the PRI multiples (next transmissions) cannot overlay the SWL at least until the SWRD. This condition identifies a region $A_{\mathrm{unf}}$ of unfeasible PRI values. Furthermore, RSs, such as RIME, have a limited number of possible parameters reconfigurations during a flyby. Thus, we identify a discrete number of PRI segments (over the flyby time), which result in a step-like function that should approximate a continuous altitude variation. Beyond the aforementioned condition, the PRI must also respect a lower bound (identified as dc limit) given by a maximum possible duty cycle (dc) and an upper bound (named Doppler limit) connected to the correct sampling of the Doppler shift ($f_D$). From Nyquist, the PRF should be at least twice the absolute Doppler variation, which depends on

the spacecraft relative velocity, i.e., [2]

$$\frac{\text{PRF}}{2} \geq f_D = \frac{2v_r}{\lambda} \sin\theta \tag{5}$$

where $\theta$ is the wave incident angle with respect to the surface normal. Since the radial component of the relative velocity is maximum at the edges of the flyby and goes to zero at the closest approach (CA), the Doppler limit increases as the Doppler shift decreases while moving closer to the CA. It is important to note that, in high-velocity flybys, there might be no available PRIs due to a too restrictive (i.e., too low) Doppler limit. To overcome this issue, the instrument can transmit a chirp with a preshift in frequency able to cancel the Doppler shift at the nadir point, removing the effect of the radial velocity and letting the PRI move in a wider range. The conditions to have valid PRIs are visually explained in Fig. 3.

The problem to address can be formulated as searching for the best sequence of PRI values that complies with both the presented timeline constraints and the mission objectives. In missions, such as JUICE, the primary objective is to acquire as much data as possible, enhancing the penetration depth and generating high-quality radargrams. However, high performances imply increasing the resource consumption in terms of data rate, resulting in a larger data volume to be transmitted to Earth. This is a critical resource in complex missions, such as JUICE, operating in the external part of the solar system. We evaluate the radar performance by estimating the signal-to-noise ratio (SNR) on the target's surface, since it is directly proportional to the pulse repetition frequency (PRF) and measures the data quality. Similarly, the data rate increases with the SWL and the PRF, but it should be minimized in accordance with the mission operational constraints. From this, one can understand that there are no solutions that enhance all the objectives simultaneously. Therefore, the goal is to explore the space of feasible solutions searching for the best trade-offs between performance and resources. As an exhaustive search of all possible parameter values cannot be performed, a strategy being able to explore the solutions space and identifying automatically the best compromises is needed.

## III. Methodology

We propose an approach to the automatic selection of the radar parameters based on multiobjective optimization, which leverages the timeline constraints and the mission requirements. The purpose is to explore the best compromises between reaching the instrument science objectives and satisfying the mission requirements by searching for the optimal set of solutions belonging to the Pareto front. In accordance with the concept of Pareto dominance in multiobjective optimization, the Pareto front represents a subset of optimal trade-off solutions among the entire population, which are considered *nondominated* in terms of joint minimization of all the objectives [5], [6]. More in detail, we need to generate a PRI segment arrangement, known also as the PRI profile, that satisfies the following conditions: the multiple-rank condition (4), the Doppler limit, and the dc limit. From a computational viewpoint, ensuring that each

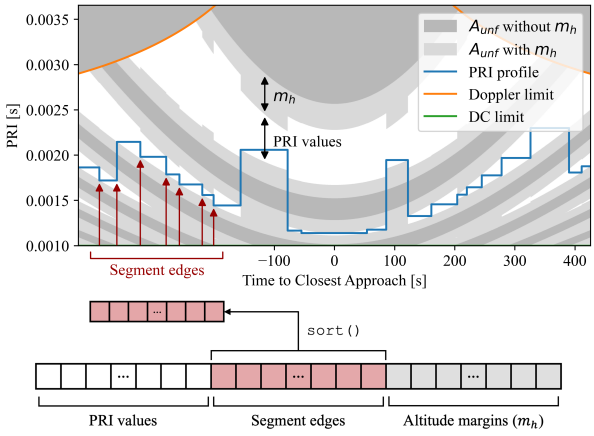


Fig. 4. Genotype representation (1-D vector) where each part encodes a property of the PRI profile. From (6), the search for the best PRI is constrained in the white space, and the condition on the PRI multiples is no longer necessary.

PRI multiple does not touch the unfeasible region can be very expensive. For this reason, we have reformulated (4) into (6)

$$\forall\ \text{rank} \in [1, r_{\max}]$$
$$\text{PRI} \notin \left[\frac{\text{SWRD} - t_s}{\text{rank}}, \frac{\text{SWRD} + \text{SWL}}{\text{rank}}\right]. \tag{6}$$

According to this formulation, the sufficient condition to have a valid PRI is that the base PRI (and not the multiples) does not intersect the replicated unfeasible regions (Fig. 4). Therefore, the search space is sharply reduced. In the case of RIME, the PRI profile is composed of a maximum of 22 segments, which are free to move in both the PRI axis and flyby time. The white space in Fig. 4 represents the feasible region where the PRI respects all the constraints. As illustrated in the figure, we opted to consider a genotype (i.e., solution encoding vector) composed of both integer and float variables. Specifically, the first part of the gene encodes the position of each segment in the PRI axis. A float number normalized in the range [0, 1] is mapped into the available PRI space in order to select a single PRI value. Subsequently, the second part of the gene selects the edges of the segments in a discretized range $[0, T_{fb}]$ that corresponds to the flyby time axis. The edges are then sorted to define the adjacent segments. Finally, the last part of the gene measures the altitude margin for each segment. In this manner, the problem is described by 65 variables, which can encode around $5^{132}$ possible solutions. It becomes now clear that an exhaustive search of all possible combinations of parameters cannot be addressed in a deterministic way.

Alternative variable representations may employ constrained optimization, for instance, by enforcing a sum constraint on the segments' lengths. However, this technique proved to be inefficient, since the equality and inequality constraints try to force the search in a space that is not intrinsically bounded. As a result, they mostly return invalid PRI profiles. For this reason, we opted for a representation where all the solutions are practicable and the goal is only to evaluate the quality of them. Concerning the objectives, we implemented a three-objective optimization, considering SNR, data rate ($R$), and altitude margin ($m_h$). From a scientific perspective, the SNR

has to be maximized, since it measures how much information the radar can collect. Thus, to achieve high values of SNR, the system should select low PRI values. The data rate instead has to be minimized to comply with the resource limitations, and it generally requires a high PRI. Finally, the altitude margin is related to the acquisition safety (or acquisition probability) that should be as high as possible. Increasing the margin means increasing the SWL and, thus, enhancing the probability of correctly sampling the echoes. However, it is important to note that a high altitude margin implies a wider unfeasible region for the PRI. Consequently, the high ranks will be disabled, and the SNR will drastically decrease.

The cost function (**F**) [5], [6] first takes as input and parses the genotype (**x**), as visually explained in Fig. 4. Then, it calculates the SWL using (1) at each rank given the assigned altitude margin. At this point, the unfeasible region is completely defined; therefore, the PRI values are selected [with (6)], and the segments are positioned. Note that, since we do not formally employ constraints to prevent the PRI from touching the unfeasible region, **F** returns a high penalty when an unviable PRI is selected, acting as a soft constraint. Finally, **F** evaluates the solution with the three objectives (SNR, data rate, and altitude margin) as follows:

$$t \in [0, T_{fb}]$$
$$\mathbf{F}(\mathbf{x}) = \left( \frac{1}{\overline{\mathrm{SNR}(t) \cdot w(t)}}, \overline{R(t) \cdot w(t)}, \frac{1}{\overline{m_h(t) \cdot w(t)}} \right). \quad (7)$$

The objectives have been computed by assuming [1]

$$\mathrm{SNR}(t) = \frac{P_S}{P_N} \cdot B_S \cdot t_s \cdot \frac{2\ \mathrm{PRF}(t)}{v_{tg}(t)} \sqrt{\frac{\lambda \cdot h(t)}{2}} \quad (8)$$

$$R(t) = \mathrm{SWL}(t) \cdot \frac{1}{t_s} \cdot \frac{\mathrm{PRF}(t)}{P_f} \cdot 2N_{\mathrm{bit}} \quad (9)$$

where $P_S$ is the signal power, $P_N$ is the noise power, $B_S$ is the signal bandwidth, $v_{tg}$ is the spacecraft tangential velocity, $P_f$ is the presumming factor, and $N_{\mathrm{bit}}$ is the number of bits used for quantization. Since the cost function needs scalar values to minimize, the objectives have been calculated on average over the entire flyby ($t \in [0, T_{fb}]$). However, there might be parts of the flyby that require particular attention, such as at the closest approach (CA) or in the presence of specific interesting targets on the ground. For this reason, to model the different conditions, we added a weighting vector $w(t)$ that balances the average while improving the performance in specific flyby segments.

As an alternative to the multiobjective approach, several techniques are available in the literature to deal with trade-off solutions within a single objective. Scalarization and $\epsilon$-constraint methods are valid approaches that, however, assume to have prior knowledge of the balance between the objectives. In our case, the trade-off solutions are unbalanced, and the single optimum is selected a posteriori, considering the resource policies among all the instruments on board the spacecraft.

## IV. Experimental Results

This section aims to present the results of the proposed approach to select the best radar parameters of RIME during the flybys on the three icy moons. As stated in the methodology formulation, the solutions represent valid radar configurations that take into account the problem constraints and ensure high system performance. Regarding the optimizer implementation, we tested several state-of-the-art algorithms based on evolutionary search and swarm intelligence. The ones oriented on collective behaviors, such as nondominated sorting PSO (NSPSO) or multiobjective hypervolume-based ACO (MHACO) [7], revealed to be rather inefficient for our problem, since they did not reach sufficient levels of convergence. Alternatively, nondominated sorting GA (NSGA-II) [5], multiobjective EA with decomposition (MOEA/D) [6], and generational MOEA/D (GMOEA/D) proved to be the most effective strategies, as they provided the best nondominated Pareto fronts in terms of objective optimality, crowding distance, convergence speed, and computational complexity. For visualization purposes, Fig. 5 shows the Pareto front obtained with the compared algorithms with only two objectives. In the following results, we adopted the GMOEA/D, considering a population of 256 elements and 10 000 iterations (2 500 000 function evaluations) for a total execution time of about 30 h (24 cores at 5.8 GHz and 128 GB of RAM). The convergence has been confirmed by a comprehensive analysis of the improvement tolerance and the population diversity.

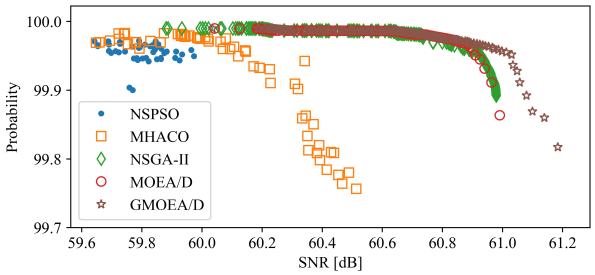


Fig. 5. Pareto front between SNR and acquisition probability obtained by different multiobjective optimization techniques (test case of the 7E1 flyby on Europa).

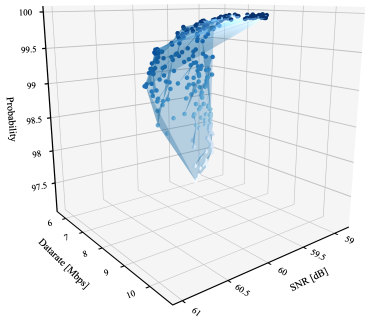


Fig. 6. Pareto front among SNR, acquisition probability, and data rate (test case of the 7E1 flyby on Europa).

Fig. 6 displays a complete example of the 3-D nondominated Pareto front among SNR, acquisition probability, and data rate. As one can see from the curved surface, the objectives confirm the relations explained in Section III. Indeed, increasing the SNR implies decreasing the altitude margin (so decreasing the acquisition probability). In other

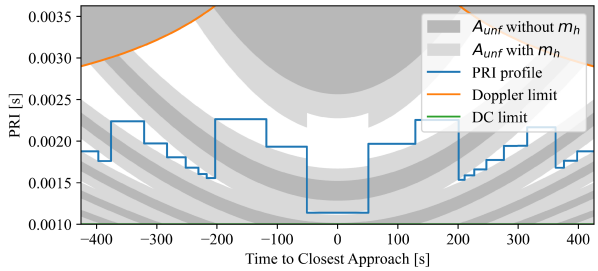


Fig. 7. Example of PRI profile (test case of the 7E1 flyby on Europa). The central segment at the CA shows the capability of the system to adaptively select the margin in order to encourage the adoption of higher ranks.

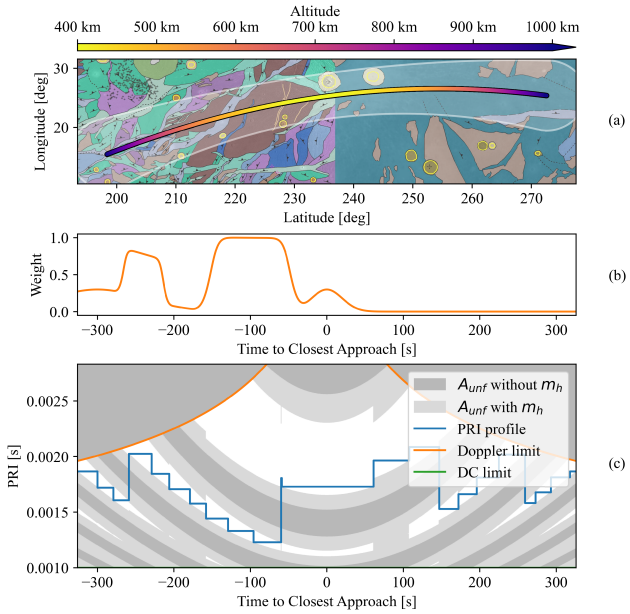


Fig. 8. Example of solution adopting weights (test case of the 2G2 flyby on Ganymede). (a) Geological map of Ganymede with the flyby position. (b) Weight values that emphasize three main ground targets. (c) PRI profile where the optimization is focused in correspondence of high weights.

words, to increase the data quality over a given performance threshold, we are forced to risk on the orbit uncertainty. The choice of the best single optimum is generally driven by the resource allocation policy among all the spacecraft's instruments. However, in the case of RIME, we consider a minimum performance threshold on the SNR below which the resource reduction cannot be accepted. Accordingly, considering the case of the 7E1 flyby on Europa, we should expect to adopt a probability of at least 99.8%, a data rate of 9 Mb/s, and a surface SNR of 60 dB.

Fig. 7 represents an example of a regular and symmetric PRI profile of a solution with high SNR. Since the PRI is always selected as the minimum, this solution provides high performance, especially at the CA. Indeed, the altitude margin of the central segment (CA) has been automatically reduced to such an extent that the instrument can operate at rank 2.

To give an example of optimization with weights, we present a solution for the 2G2 flyby on Ganymede. Fig. 8 shows this case, considering three interesting ground targets to which the weighting vector devotes particular attention. As a result, in correspondence to high values of weights, the PRI is minimized, enhancing the SNR on the first part of the flyby.

## V. Discussion and Conclusion

In this letter, we have proposed a novel semiautomatic approach to configure RS parameters during flybys. We considered a nadir-looking monostatic RS with SAR and employed multiple ranks to improve the signal-to-noise ratio. The rapid change in altitude of the spacecraft generates a complex unfeasible region for the PRI selection. To comply with all the constraints, an ad hoc variable representation has been designed. Then, a multiobjective optimization allowed us to find optimal (i.e., nondominated) trade-off solutions capable of addressing both the instrument scientific requirements and the mission constraints. The simulation results identify excellent solutions with regular and symmetric PRI profiles. The approach also allows one to define different weight values for giving importance to different flyby segments, thus concentrating the resources on particularly interesting ground targets. Future improvements concern the possible integration in the multiobjective optimization of other radar parameters, such as the pulsewidth. Increasing the number of degrees of freedom will make the search more difficult but can result in better solutions, enhancing the system performance.

As a final remark, although the presented approach has been tested on an RS, it is also suitable both for other radar systems and other types of instruments. Indeed, once the instrument behavior during a flyby has been defined, the parameters can be easily encoded into a genotype, and the optimization works identically by improving the selected mission objectives.

## References

[1] G. Picardi et al., "The Mars advanced radar for subsurface and ionosphere sounding (MARSIS): Concept and performance," in *Proc. IEEE Int. Geosci. Remote Sens. Symp. (IGARSS)*, vol. 5, Jun. 1999, pp. 2674–2677.

[2] R. Croci, R. Seu, E. Flamini, and E. Russo, "The SHAllow RADar (SHARAD) onboard the NASA MRO mission," *Proc. IEEE*, vol. 99, no. 5, pp. 794–807, May 2011.

[3] L. Bruzzone et al., "RIME: Radar for icy Moon exploration," in *Proc. IEEE Int. Geosci. Remote Sens. Symp. (IGARSS)*, Jul. 2013, pp. 3907–3910.

[4] A. Heske, "Science and payloads for the next decades of ESA's cosmic vision program," in *Proc. IEEE Aerosp. Conf.*, Mar. 2016, pp. 1–13.

[5] K. Deb, A. Pratap, S. Agarwal, and T. Meyarivan, "A fast and elitist multiobjective genetic algorithm: NSGA-II," *IEEE Trans. Evol. Comput.*, vol. 6, no. 2, pp. 182–197, Apr. 2002.

[6] Q. Zhang and H. Li, "MOEA/D: A multiobjective evolutionary algorithm based on decomposition," *IEEE Trans. Evol. Comput.*, vol. 11, no. 6, pp. 712–731, Dec. 2007.

[7] G. Acciarini, D. Izzo, and E. Mooij, "MHACO: A multi-objective hypervolume-based ant colony optimizer for space trajectory optimization," in *Proc. IEEE Congr. Evol. Comput. (CEC)*, Jul. 2020, pp. 1–8.

Open Access funding provided by 'Università degli Studi di Trento' within the CRUI CARE Agreement